

**Cyclic Voltammetric Study of Some Anti-Chagas Active Quinoxaline 1,4-Di-N-Oxide-2-Ketone Derivatives**

**Silvia Pérez-Silanes<sup>1</sup>, Goutham Devarapally<sup>2</sup>, Enrique Torres<sup>1</sup>, Elsa Moreno<sup>1</sup>, Ignacio Aldana<sup>1</sup>, Antonio Monge<sup>1</sup> and Philip W. Crawford<sup>2\*</sup>.**

<sup>1</sup> *Neglected Diseases Section. Instituto de Salud Tropical, University of Navarra, C/ Irunlarrea 1, 31008 Pamplona, Spain.*

<sup>2</sup> *Department of Chemistry, Southeast Missouri State University, Cape Girardeau, Missouri 63701, USA.*

\*Author to whom correspondence should be addressed: Department of Chemistry, MS6400, Southeast Missouri State University, Cape Girardeau, Missouri, 63701, U.S.A; 573-651-2166 (phone); 573-651-2508 (fax); pcrawford@semo.edu

## ABSTRACT

The electrochemical properties of 24 quinoxaline 1,4-di-*N*-oxide-2-ketone derivatives with varying degrees of anti-chagas activity were investigated in the aprotic solvent dimethylformamide (DMF) using cyclic voltammetry and first derivative cyclic voltammetry. For this group of compounds, the first reduction in DMF was either reversible or quasireversible and consistent with reduction of the *N*-oxide functionality to form the radical anion. The second reduction process for these compounds was found to be irreversible under the conditions used. The reduction potentials correlated well with molecular structure. Substitution in the 3-, 6-, and 7- positions of the quinoxaline ring by electron-withdrawing substituents directly affects the ease of reduction and improves the biological activities of these compounds, whereas substitution by electron-donating groups has the opposite effect. The results of this study when combined with previous work into their mechanism of action against chagas disease suggest that charge transfer might play a role in the mechanism of action for these compounds.

Keywords: quinoxaline-di-*N*-oxide-2-ketones, cyclic voltammetry, anti-chagas activity, reduction potential

## INTRODUCTION

Chagas' disease continues to represent a health threat for an estimated 8 million people, the majority of whom live in Latin America [1]. Although more than 100 years have elapsed since the discovery of this disease, the discovery of a valid chemotherapy treatment for Chagas' disease is still an open field and remains an unsolved problem. Early experiments carried out on one of the main drugs used for treating Chagas, Nifurtimox (Nfx), suggest that intracellular reduction followed by redox cycling, yielding reactive oxygen species (ROS), may be the major mode of action of Nfx against *T. cruzi*. ROS can cause direct cellular damage by reacting with various biological macromolecules, or indirect cellular damage by the generation of the highly reactive hydroxyl radical via Haber–Weis and Fenton reactions [2,3].

It is well-known that some quinoxaline *N,N*-dioxides are species that suffer a bioreductive process in hypoxic conditions, producing hydroxyl radical and quinoxaline. Quinoxalines could produce parasitic damage through the production of radical species affecting the redox metabolism [4]. As previously observed [5], the absence of the *N*-oxide moiety produces a decrease in the antiepipimastigote activity, confirming that this group plays a key role in the mechanism of quinoxaline di-*N*-oxide antitrypanosomal activity.

In the search for more selective and less toxic anti-chagasic drugs, we have developed new quinoxaline derivatives possessing the di-*N*-oxide moiety as the bioreductive pharmacophore [6]. In this publication, we have demonstrated that our quinoxaline derivatives affect the mitochondrial dehydrogenase activity [6]. Therefore, electrochemistry plays an important role when studying the formation of this radical species and its reactivity in one-pot systems [7]. The purpose of the present study was to investigate the electrochemical properties of a series of quinoxaline-di-*N*-oxide-2-

ketone derivatives, and determine the possible relationship between their reduction potentials, their structure and their anti-chagasic activity.

## **EXPERIMENTAL**

### ***Chemical synthesis and anti-Chagas activity***

The compounds presented in this paper, along with their structures, are shown in Table 1. The methods for the synthesis of quinoxaline-1,4-di-*N*-oxide-2-ketone derivatives were previously reported [6].

### ***Pharmacology***

The anti-*T. cruzi* activity of the quinoxaline-1,4-di-*N*-oxide-2-ketone derivatives presented in this study was tested *in vitro* against the epimastigote form of *T. cruzi*, Tulahuén 2 strain, as previously described [6]. The existence of the epimastigote form of *T. cruzi* as an obligate mammalian intracellular stage has been revised and confirmed [8]. The compounds were incorporated into the biological media at 25  $\mu$ M and their ability to inhibit growth of the parasite was evaluated in comparison to the control (no drug added to the media) at day 5. Nfx was used as the reference trypanosomicidal drug. The percentage of growth inhibition (PGI) and the inhibitory concentration 50% ( $\mu$ M) against *T. Cruzii* values ( $IC_{50}$ ) were calculated as indicated in Table 1.

### ***Electrochemistry***

Test solutions contained 1.0 mM of the quinoxaline compound and 0.10 M tetrabutylammonium perchlorate (TBAP). Test solutions were deaerated for 15 minutes prior to obtaining the electrochemical data by passing a gentle stream of prepurified dinitrogen through the solution. A dinitrogen atmosphere was maintained over the test solution during all experiments. Cyclic voltammetric measurements were carried out using a CHI Instruments 630 voltammetric analyzer. Solution resistance was uncompensated. The electrodes consisted of a Pt-disk (1.6 mm diameter) electrode, a Pt-wire auxiliary electrode, and a Ag/AgNO<sub>3</sub> (0.1 M in acetonitrile) reference electrode.

Scan rates ranged from 0.1 V/s to 1 V/s. Half-wave potentials and the difference in peak potentials were calculated using the following equations, respectively [9]:  $E_{1/2} = (E_{pa} + E_{pc})/2$  and  $\Delta E_p = E_{pa} - E_{pc}$ . For first derivative cyclic voltammograms,  $E_{pc}$  was measured at the point where the derivative curves crossed the baseline [9]. To account for daily variations in the reference electrode and liquid junction potentials, ferrocene (Fc) was added to each solution following measurements of the test compound, and used as an internal reference redox system [10]. All potentials are reported versus the ferrocene/ferrocinium (Fc/Fc<sup>+</sup>) redox couple, i.e.  $E_{pc, SRE} - E_{1/2, Fc/Fc^+}$  or  $E_{1/2, SRE} - E_{1/2, Fc/Fc^+}$ . Half-wave potentials ( $E_{1/2}$ ) for ferrocene varied from -0.0095 V to 0.0485 V during the course of this study. Peak currents were measured from the extrapolated baselines for both the cathodic and anodic processes [11]. Dimethylformamide (DMF) (Fisher Scientific) was used as the solvent and TBAP (Aldrich Chemical Company) served as the supporting electrolyte. Ferrocene were obtained from Aldrich Chemical Company. All reagents were obtained in the highest purity available and used without further purification.

## RESULTS AND DISCUSSION

### *Electrochemical behavior*

The present study included a series of 24 quinoxaline 1,4-di-*N*-oxide-2-ketone derivatives. The electrochemical properties of these derivatives were studied using cyclic voltammetry and first derivative cyclic voltammetry in DMF with TBAP as supporting electrolyte. The structures and summary data for these compounds are provided in Tables 1 to 3, and representative voltammograms are shown in Figures 1 and 2. Hammett plots are provided in Figure 3. All reductions were diffusion controlled, as indicated by fairly constant current functions at varying scan rates for each derivative [9,11].

For all the quinoxaline di-*N*-oxide derivatives studied, the first cyclic voltammetric wave observed during the reduction was either reversible or quasireversible (Figures 1a

and 2a). Values of  $\Delta E_p$  (65 to 81 mV at 0.1 V/s) and  $E_{pc}-E_{1/2}$  (-32.5 to -40.5 mV at 0.1 V/s) for this redox couple were reasonably close to theoretical for a reversible, one electron transfer, i.e. 59 mV for  $\Delta E_p$  and -28.5 mV for  $E_{pc}-E_{1/2}$  [11]. In addition,  $i_{pa}/i_{pc}$  values calculated for the first voltammetric wave were close to unity ( $i_{pa}/i_{pc} = 0.65$  to 0.97) at all scan rates for all derivatives but compounds **4** and **17** ( $i_{pa}/i_{pc} = 0.44$  and 0.52, respectively), indicating the absence of significant kinetic or other complications in the electrode process [11]. Thus, the reduction product for this redox couple appeared fairly stable on the experimental time scale for these derivatives. This is further supported by multiple scans of the first voltammetric wave, which show no changes in the reversibility of this electrode process upon redox cycling (Figures 1b and 2b). The first voltammetric wave observed is consistent with the reversible reduction of the *N*-oxide functionality to a radical anion, in conjunction with other studies of the electrochemical behavior of quinoxaline di-*N*-oxides in DMF [12-16]. In fact, reduction of quinoxaline 1,4-di-*N*-oxide in DMF has been shown via ESR and electrochemistry to involve one-electron reduction of the nitron to the radical anion [15]. A second, irreversible voltammetric wave was observed for all derivatives at potentials between -1.7 and -2.4 V (Tables 2 and 3, Figures 1c and 2c), and is attributed to formation of the dianion [17]. The irreversibility of this voltammetric wave might be due to a following chemical reaction, i.e. an EEC mechanism. A third irreversible voltammetric wave was observed at potentials negative of -2.1 V for all compounds studied with the exception of compound **21**. This electrode process could be due to reduction of the group at position 2 of the quinoxaline ring. In some cases, the second and third reduction waves were close together so that one of the waves appeared as a shoulder to the other. For some of the compounds, a fourth voltammetric process negative of the third reduction process was evident in the voltammograms. The second, third, and fourth reduction processes were not investigated in further detail.

For derivative **12**, multiple scans between -0.4 and -2.8 V resulted in the observation of a new redox couple negative of the voltammetric wave for the formation of the radical anion (Figure 2d). Since this electrode process appeared between the first and third voltammetric waves following redox cycling, mechanistically it is attributed to the product formed via a chemical step that follows the third voltammetric wave.

### ***Relationship between electrochemical behavior and structure***

Examination of the data for the first voltammetric wave and the anti-chagas activity data indicates that structure influences both the reduction potentials and activities of these compounds (e.g. Tables 1 and 2, Figure 3). The effects of incorporating an electron-withdrawing group (i.e. chloro, fluoro, difluoromethyl, and trifluoromethyl) or an electron-releasing group (i.e. methyl and methoxy) onto the conjugated quinoxaline ring have been reported in previous studies [7, 12, 13, 14, 16, 17, 18]. The present study correlates well with these earlier reports on the structural effects on potential. Substitution of a single electron-withdrawing group on the quinoxaline ring system at position 3 resulted in a positive shift in reduction potential and in an increase in the activity. For example, replacing the 3-methyl group in compound **6** with the difluoromethyl group in compound **14** and the trifluoromethyl group in compound **10** results in positive shifts in  $E_{1/2}$  of 0.146 V and 0.238 V, respectively. The anti-chagas activities of these three derivatives follows the same order, i.e. compound **10** is the most active and compound **6** is the least active. Other examples include derivatives **7** vs. **11**, and derivatives **8** vs. **13**. The same effect resulted when similar substitutions were made at positions 6 or 7 (cf. compounds **6** vs. **8**, **10** vs. **13**, and **14** vs. **16** vs. **17** vs. **18**) whereas an electron-donating group in these positions resulted in a more hindered reduction and generally decreased activity. For example, replacing the hydrogen atom in the 7-position in compound **6** with the methoxy group in compound **9** and the methyl group in compound **7** results in shifts in  $E_{1/2}$  of -0.027 V and -0.034 V, respectively. These decreases in potential are accompanied

by concurrent decreases in the activities of these three compounds. Other examples include derivatives **10** vs. **11** vs. **12**, and derivatives **14** vs. **15** vs. **16**. In addition, substitution of a second electron-withdrawing chloro group onto the quinoxaline ring enhanced the positive shift in potential and in activity (cf. **16** vs. **17**), coinciding with a previously reported study [16]. These results are consistent with facilitation of quinoxaline reduction by a positive charge at the reaction site [18]. This is further demonstrated by Figure 3, which shows that the reduction potentials for the quinoxaline derivatives within various analogues generally fit the modified Hammett equation,  $\Delta E_{1/2} = \rho_{\pi R} \sigma_x$  (correlation coefficients ranged from 0.98 to 0.99), where  $\sigma_x$  is the polar inductive electronic substituent constant taken as the average of the sum of  $\sigma_m$  and  $\sigma_p$  (Table 4, [19]) and  $\rho$  is the reaction constant [18, 20]. Comparison of the data in Tables 1 and 2 demonstrates that the substituent group at R<sub>2</sub> has relatively little effect on reduction potential, presumably due to the distance from the site of reduction.  $E_{1/2}$  values for compounds **3** to **5** cover a range of only 0.005 V, and those for compounds **13** and **19** to **22** span a range of only 0.020 V from most positive to most negative.

The data suggest that a relationship between reduction potential and activity for these quinoxaline derivatives is possible. In this case, bioreductive activation would generally be expected to be more facile for the more easily reduced derivatives. In general, upon comparing the activity data with the reduction potential data presented in Table 1, it can be observed that the most active compounds, with a PGI of 100% and IC<sub>50</sub> below that of the drug Nfx, are those that have the least negative reduction potentials. The three compounds with activities well below a PGI of 100%, i.e. compounds **6**, **7**, and **9**, all have half-wave potentials more negative than -1.5 V (versus Fc/Fc<sup>+</sup>). Likewise, compounds **6** and **7** have IC<sub>50</sub> values above 25  $\mu$ M. (The IC<sub>50</sub> value of derivative **9** was not measured.) Most of the derivatives possessing either a trifluoromethyl or difluoromethyl group in position 3 have potentials well positive of the

most easily reduced and biologically active 3-methyl derivative, i.e. compound **1**, and are generally much more active than 3-methyl derivatives **6** to **9**. In a previous study, we were able to demonstrate that mitochondrial dehydrogenases are involved in the anti-*T. cruzi* activity of the most active derivatives [6]. Specifically, derivatives **3** and **13** decreased mitochondrial dehydrogenases activity in the parasites and demonstrated better animal survival percentages in the Y-infected mice than with Benznidazole. Thus, it is conceivable that the redox behavior of these quinoxaline derivatives is important to their mechanism of action. However, a direct correlation between anti-chagas activity and potential for all the derivatives used in this study combined was not observed when taken together. The fact that certain exceptions exist in the data, cf. derivatives **4** and **5**, indicates that redox behavior alone cannot be used to explain the activities observed for these compounds. Obviously, electrochemical data should be interpreted with some degree of caution. Aside from bioreduction, factors such as lipophilicity, diffusion, stereochemistry, solubility, metabolism, absorption or site binding, and bioactivation must also be considered when determining the *in vivo* mechanism of action of anti-chagasic compounds. A detailed study of the mode of action of the quinoxaline-1,4-di-*N*-oxide-2-ketone derivatives is beyond the scope of this paper, and the exact mechanism of action remains unclear at this point. Never-the-less, the results presented above indicate that the quinoxaline *N*-oxide system constitutes a starting point for further chemical modifications in order to improve the *T. cruzi* activity via a possible bioreduction mechanism, and support further *in vivo* studies of these compounds in animal models of Chagas' disease.

## **ACKNOWLEDGMENTS**

This work has been carried out with the financial support of the PIUNA project and with the help of FIMA (Fundación para la Investigación Médica Aplicada) from the University of Navarra. E. Torres is indebted to the University of Navarra for a grant.

## REFERENCES

- [1] J. R. Anis Rassi, J. A. Marin-Neto, *Lancet* **2010**, 375, 1388.
- [2] S. N. Moreno, R. P. Mason and R. Docampo, *J. Biol. Chem.* 1984, 259, 5606.
- [3] C. Olea-Azar, C. Rigol, F. Mendizabal, A. Morello, J.D. Maya, C. Moncada, E. Cabrera, R. Di Maio, M. González and H. Cerecetto, *Free Radic. Res.* **2003**, 37, 993.
- [4] V. Junnotula, A. Rajapakse, L. Arbillaga, A. López de Cerain, B. Solano, R. Villar, A. Monge, K. S. Gates, *Bioorg. Med. Chem.* **2010**, 18, 3125.
- [5] L. Boiani, H. Cerecetto, M. González, M. Risso, C. Olea-Azar, O. E. Piro, E. E. Castellano, A. López de Ceráin, O. Ezpeleta, A. Monge, *Eur. J. Med Chem.* **2001**, 36, 771.
- [6] D. Benitez, M. Cabrera, P. Hernández, L. Boiani, M. L. Lavaggi, R. Di Maio, G. Yaluff, E. Serna, S. Torres, M. E. Ferreira, N. Vera de Bilbao, E. Torres, S. Pérez-Silanes, B. Solano, E. Moreno, I. Aldana, A. López de Ceráin, H. Cerecetto, M. González, A. Monge, *J. Med. Chem.* **2011**, 54, 3624.
- [7] J.A. Squella, S. Bollo, L.J. Núñez-Vergara, *Curr. Org. Chem.* **2005**, 9 (6), 565.
- [8] M. Almeida-de-Faria, E. Freymuller, W. Colli, M. J. Alves, *Exp. Parasitol.*, **1999**, 92, 263.
- [9] P.H. Rieger, *Electrochemistry*, 2nd edition, Chapman and Hall, New York, 1994.
- [10] G. Gritzner, J. Kuta, *Pure Appl. Chem.*, **1984**, 56, 461.
- [11] A.J. Bard, L.R. Faulkner, *Electrochemical Methods: Fundamentals and Applications*, 2<sup>nd</sup> ed., Wiley, New York, 2001.
- [12] M.D. Ryan, R.G. Scamehorn, P. Kovacic, *J. Pharmaceut. Sci.* **1985**, 74, 492.
- [13] P.W. Crawford, R.G. Scamehorn, U. Hollstein, M.D. Ryan, P. Kovacic, *Chem.-Biol. Interact.* **1986**, 60, 67.
- [14] J.R. Ames, M.A. Houghtaling, D.L. Terrian, *Electrochim. Acta* **1992**, 37, 1433.
- [15] H. Miyazaki, Y. Matsuhisa, T. Kubota, *Bull. Chem. Soc. Jpn.* **1981**, 54, 3850.

- [16] E. Moreno, S. Pérez-Silanes, S. Gouravaram, A. Macharam, S. Ancizu, E. Torres, I. Aldana, A. Monge, P.W. Crawford, *Electrochim. Acta* **2011**, *56*, 3270.
- [17] K.R. Barqawi, M.A. Atfah, *Electrochim. Acta* **1987**, *32*, 597.
- [18] P. Zuman, *Substituent Effects in Organic Polarography*, Plenum Press, New York (1967).
- [19] C. Hansch, A. Leo, R.W. Taft, *Chem. Rev.* **1991**, *91*, 165.
- [20] M. P. Strier, J. C. Cavagnol, *J. Am. Chem. Soc.* **1958**, *80*, 1565.

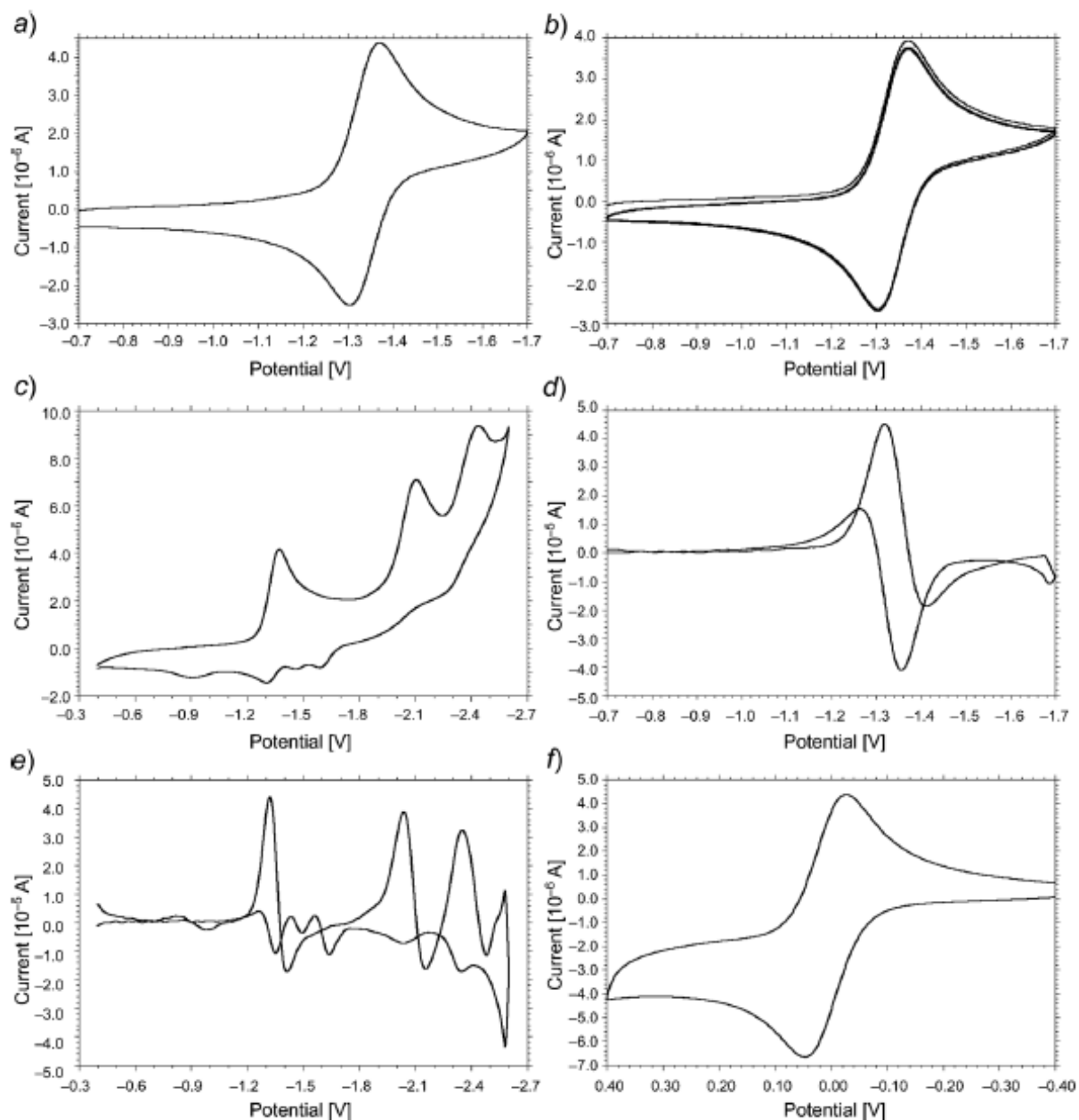


Fig. 1. Cyclic voltammetric reduction of [1,4-dioxido-3-(trifluoromethyl)quinoxalin-2-yl](4-phenylpiperazin-1-yl)methanone (**24**) in DMF at 100 mV/s ( $E$  vs. (Ag/AgNO<sub>3</sub>)/V): a) single scan between -0.7 and -1.7 V, b) multiple scans between -0.7 and -1.7 V, c) single scan between -0.4 and -2.6 V, d) first-derivative cyclic voltammogram between -0.7 and -1.7 V, e) first-derivative cyclic voltammogram between -0.4 and -2.6 V, and f) cyclic voltammogram for the ferrocene redox couple used as a reference for peak-potential determination.

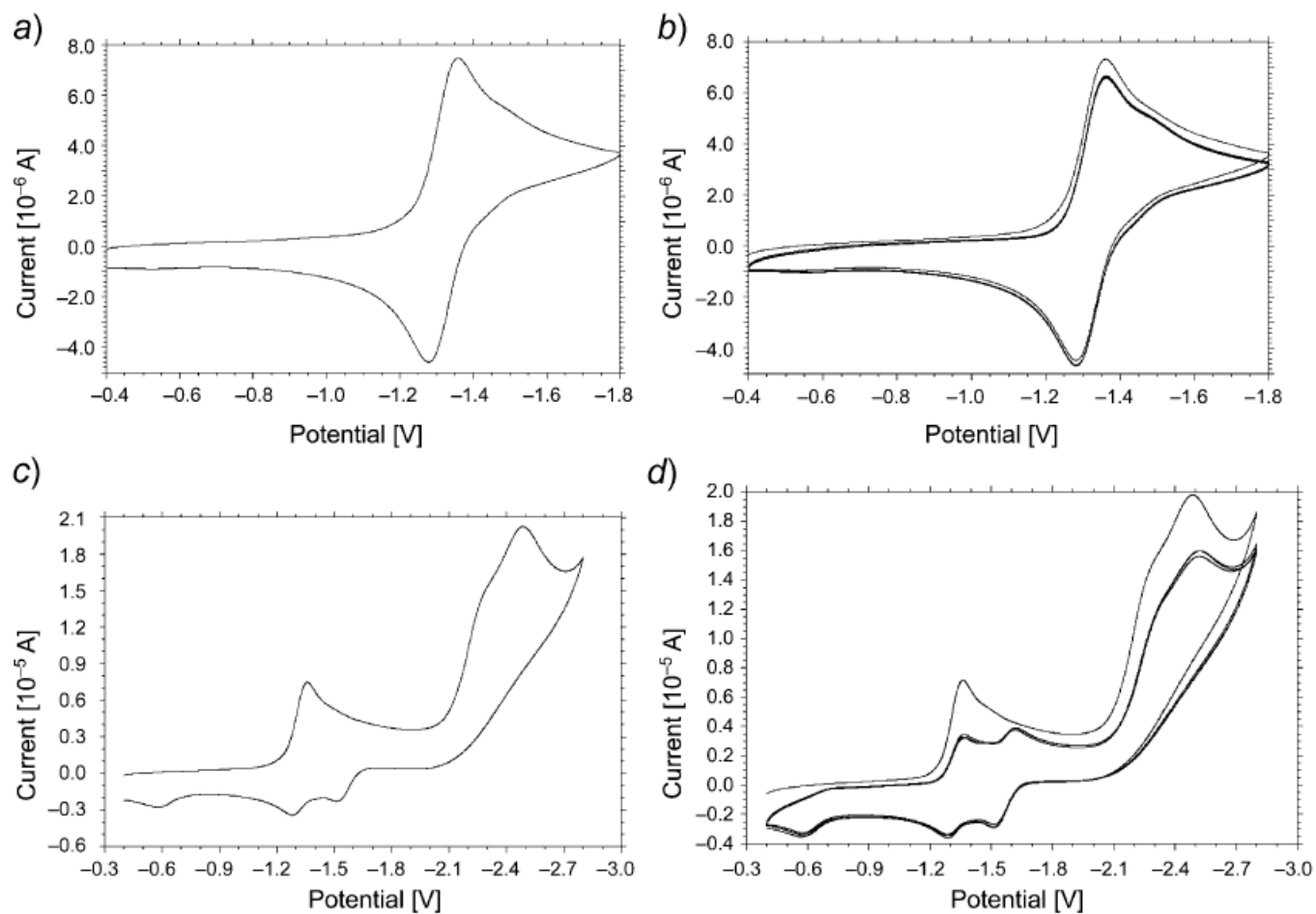


Fig. 2. Cyclic voltammetric reduction of [7-methoxy-1,4-dioxido-3-(trifluoromethyl)quinoxalin-2-yl]phenylmethanone (**12**) in DMF at 100 mV/s ( $E$  vs. (Ag/AgNO<sub>3</sub>)/V): a) single scan between -0.4 and -1.8 V, b) multiple scans between -0.4 and -1.8 V, c) single scan between -0.4 and -2.8 V, and d) multiple scans between -0.4 and -2.8 V.

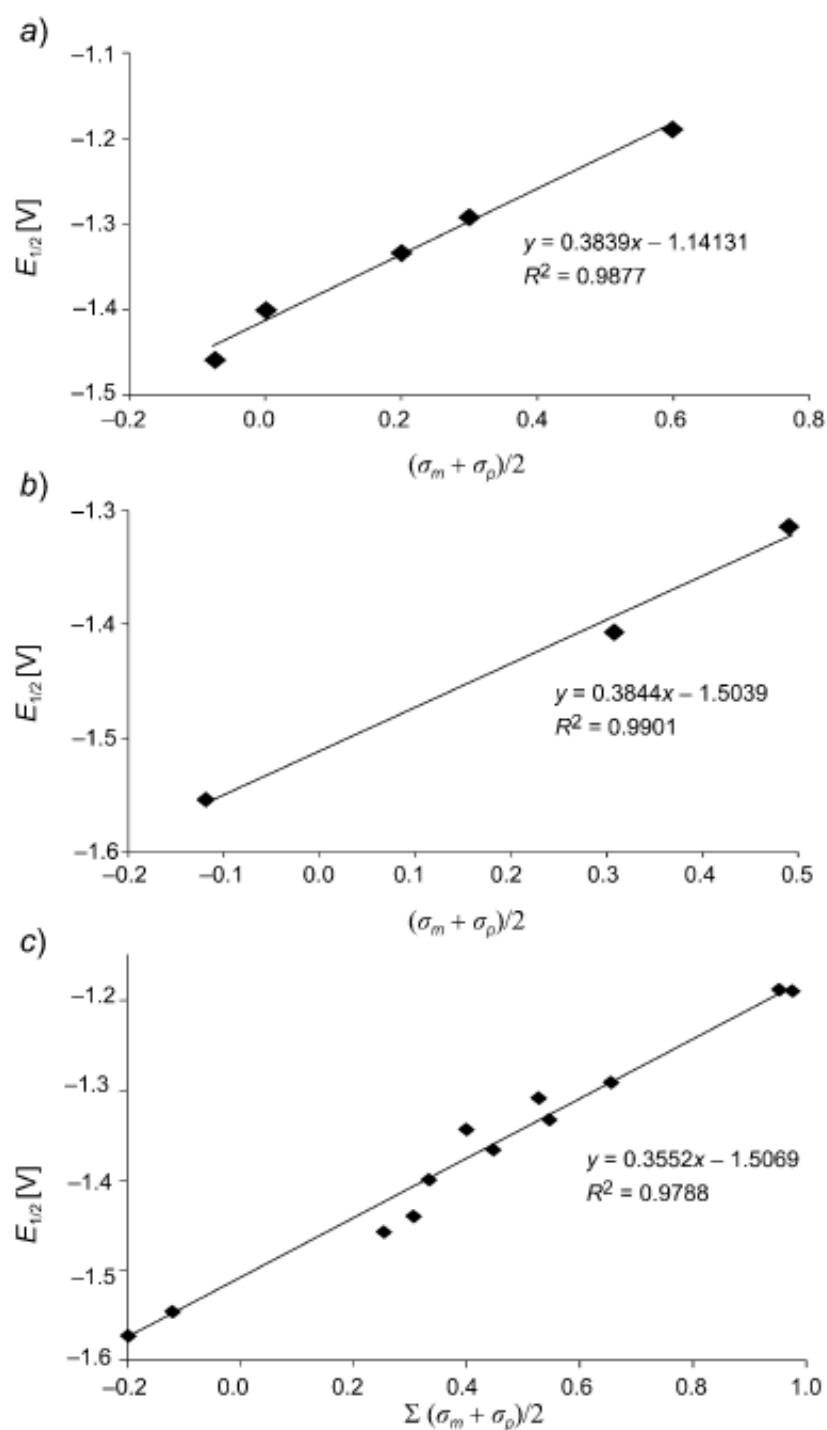
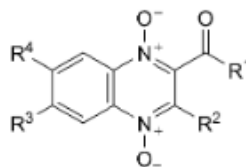


Fig. 3. Plot of a) half-wave potential ( $E_{1/2}$  vs.  $\text{Fc}/\text{Fc}^+$ ) vs.  $(\sigma_m + \sigma_p)/2$  for substituent groups  $R^3$ -/ $R^4$ - of compounds **14**–**18**; b) half-wave potential ( $E_{1/2}$  vs.  $\text{Fc}/\text{Fc}^+$ ) vs.  $(\sigma_m + \sigma_p)/2$  for substituent group  $R^2$  of **6**, **10**, and **14**, and c) half-wave potential ( $E_{1/2}$  vs.  $\text{Fc}/\text{Fc}^+$ ) vs.  $\Sigma(\sigma_m + \sigma_p)/2$  for substituent groups  $R^2$  and  $R^3$ / $R^4$  of compounds **6**–**18**

Table 1. Structure, Cyclic Voltammetric Data, and Anti-Chagas Activity of the 1,4-Dioxidoquinoxalin-2-yl Ketone Derivatives **1–24**



	R <sup>1</sup>	R <sup>2</sup>	R <sup>3</sup>	R <sup>4</sup>	Cyclic voltammetry <sup>a)</sup>			Anti-Chagas activity <sup>b)</sup>	
					$i_{pa}/i_{pc}$	$E_{1/2}$ [V]	$\Delta E_p$ [V]	PGI [%] <sup>c)</sup>	IC <sub>50</sub> [ $\mu$ M] <sup>d)</sup>
<b>1</b>	Me	Me	F	F	0.722	-1.418	0.072	100	0.4
<b>2</b>	Et	CF <sub>3</sub>	Cl	Cl	0.901	-1.093	0.065	100	0.78
<b>3</b>	Me	CF <sub>3</sub>	F	F	0.829	-1.179	0.069	100	0.032
<b>4</b>	<sup>i</sup> Pr	CF <sub>3</sub>	F	F	0.436	-1.181	0.076	23	>25
<b>5</b>	<sup>t</sup> Bu	CF <sub>3</sub>	F	F	0.916	-1.176	0.075	30	4.9
<b>6</b>	Ph	Me	H	H	0.672	-1.546	0.069	19	>25
<b>7</b>	Ph	Me	H	Me	0.724	-1.580	0.065	8	>25
<b>8</b>	Ph	Me	F	F	0.748	-1.442	0.071	92	4.2
<b>9</b>	Ph	Me	H	MeO	0.685	-1.573	0.075	9	
<b>10</b>	Ph	CF <sub>3</sub>	H	H	0.926	-1.308	0.066	100	0.9
<b>11</b>	Ph	CF <sub>3</sub>	H	Me	0.804	-1.344	0.065	99	1.3
<b>12</b>	Ph	CF <sub>3</sub>	H	MeO	0.838	-1.366	0.081	98	
<b>13</b>	Ph	CF <sub>3</sub>	F	F	0.867	-1.188	0.069	100	0.7
<b>14</b>	Ph	CHF <sub>2</sub>	H	H	0.884	-1.400	0.069	36	>25
<b>15</b>	Ph	CHF <sub>2</sub>	H	MeO	0.971	-1.458	0.069	100	10
<b>16</b>	Ph	CHF <sub>2</sub>	H	Cl	0.922	-1.291	0.068	100	6.4
<b>17</b>	Ph	CHF <sub>2</sub>	Cl	Cl	0.515	-1.189	0.072	100	4.7
<b>18</b>	Ph	CHF <sub>2</sub>	H	F	0.763	-1.334	0.072	100	6.3
<b>19</b>	naphthalen-1-yl	CF <sub>3</sub>	F	F	0.889	-1.196	0.073	100	3.9
<b>20</b>	furan-2-yl	CF <sub>3</sub>	F	F	0.910	-1.183	0.071	100	5.2
<b>21</b>	thiophen-2-yl	CF <sub>3</sub>	F	F	0.792	-1.190	0.072	100	2.8
<b>22</b>	4-chlorophenyl	CF <sub>3</sub>	F	F	0.934	-1.176	0.073	100	2.5
<b>23</b>	4-(4-chlorophenyl)piperazin-1-yl	CF <sub>3</sub>	H	H	0.647	-1.341	0.066	100	0.79
<b>24</b>	4-phenylpiperazin-1-yl	CF <sub>3</sub>	H	H	0.846	-1.349	0.066	100	0.76
	Nfx							100	7.7

<sup>a)</sup> Substrate, 1.0 mM; (Bu<sub>4</sub>N)ClO<sub>4</sub>, 0.10M; DMF; Pt working electrode; Ag/AgNO<sub>3</sub> reference electrode; Pt-wire counter electrode; 100 mV/s; r.t.;  $E$  vs. (Fc/Fc<sup>+</sup>)/V; currents reported in  $\mu$ A. <sup>b)</sup> *T. cruzi* antiproliferative activity of quinoxaline *N,N*-dioxides and nifurtimox (Nfx) as reference drug. <sup>c)</sup> Percentage of growth inhibition; inhibition of epimastigote growth of Tulahuen 2 strain, dose = 25  $\mu$ M. The results are the mean of three independent experiments with a SD less than 10% in all cases. <sup>d)</sup> IC<sub>50</sub> = Inhibitory concentration (50%) [ $\mu$ M] against *T. cruzi*.

Table 2. *First-Derivative Voltammetric Data of the 1,4-Dioxidoquinoxalin-2-yl Ketone Derivatives 1–24<sup>a)</sup>*

	1st Derivative <sup>b)</sup>					
	$E_{pc,1}$	$E_{pa,1}$	$E_{1/2,1}$	$E_{pc,2}$	$E_{pc,3}$	$E_{pc,4}$
<b>1</b>	–1.466	–1.394	–1.430	–2.002	–2.264	–2.474
<b>2</b>	–1.128	–1.058	–1.093	–1.861	–2.122	–2.329
<b>3</b>	–1.213	–1.142	–1.178	–1.925	–2.090	–2.273
<b>4</b>	–1.220	–1.139	–1.180	–1.907	–2.138	–
<b>5</b>	–1.212	–1.138	–1.175	–1.957	–2.222	–2.519
<b>6</b>	–1.579	–1.508	–1.544	–2.020	–2.161	–2.193
<b>7</b>	–1.614	–1.545	–1.580	–2.045	–2.180	–2.221
<b>8</b>	–1.481	–1.405	–1.443	–1.921	–2.127	–2.267
<b>9</b>	–1.611	–1.534	–1.573	–2.025	–2.235	–
<b>10</b>	–1.342	–1.270	–1.306	–2.083	–2.259	–
<b>11</b>	–1.379	–1.307	–1.343	–2.076	–2.154	–2.252
<b>12</b>	–1.408	–1.326	–1.367	–2.386	–2.534	–
<b>13</b>	–1.227	–1.153	–1.190	–1.923	–2.068	–2.207
<b>14</b>	–1.437	–1.364	–1.401	–2.003	–2.090	–2.197
<b>15</b>	–1.493	–1.420	–1.457	–2.019	–2.095	–2.253
<b>16</b>	–1.327	–1.254	–1.291	–1.978	–2.097	–
<b>17</b>	–1.226	–1.152	–1.189	–1.874	–2.073	–2.231
<b>18</b>	–1.369	–1.295	–1.332	–1.976	–2.148	–2.457
<b>19</b>	–1.232	–1.160	–1.196	–1.923	–	–
<b>20</b>	–1.220	–1.144	–1.182	–1.924	–2.058	–
<b>21</b>	–1.228	–1.154	–1.191	–1.909	–	–
<b>22</b>	–1.215	–1.139	–1.177	–1.921	–2.155	–2.330
<b>23</b>	–1.376	–1.308	–1.342	–2.065	–2.382	–
<b>24</b>	–1.383	–1.313	–1.348	–2.118	–2.449	–

<sup>a)</sup> Substrate, 1.0 mM; (Bu<sub>4</sub>N)ClO<sub>4</sub>, 0.10M; DMF; Pt working electrode; Ag/AgNO<sub>3</sub> reference electrode; Pt wire counter electrode; 100 mV/s; r.t.;  $E$  vs. (Fc/Fc<sup>+</sup>)/V; currents reported in  $\mu$ A. <sup>b)</sup>  $E_{pc}$  and  $E_{pa}$  determined at the point where the derivative curve crosses the baseline [9].

Table 3. Cyclic Voltammetric Data of the 1,4-Dioxidoquinaxalin-2-yl Ketone Derivatives<sup>a)</sup>

	$E_{\text{red}} [\text{V}]$	$E_{\text{pot}} [\text{V}]$	$E_{\text{ox}} [\text{V}]$	$i_{\text{pa}} [\mu\text{A}]$	$i_{\text{pc}} [\mu\text{A}]$	$i_{\text{pa}}/i_{\text{pc}}$	$\Delta E_p [\text{V}]$	$E_{\text{pc}} - E_{\text{ox}} [\text{V}]$	$E_{\text{pc}} - E_{\text{red}} [\text{V}]$	$n^b$	$i_{\text{pc}} \nu^{1/2} C$	$E_{\text{pc}}^c [\text{V}]$	$i_{\text{pc}} [\mu\text{A}]$	$E_{\text{pc}}^d [\text{V}]$	$i_{\text{pc}} [\mu\text{A}]$
1	-1.454	-1.382	-1.418	4.58	3.31	0.722	0.072	-0.036	-0.036	0.792	0.01448	-1.988	4.86	-2.251	4.70
2	-1.126	-1.061	-1.093	3.60	3.25	0.903	0.065	-0.033	-0.033	0.88	0.01138	-1.846	3.56	-2.109	2.68
3	-1.213	-1.144	-1.179	4.13	3.42	0.829	0.069	-0.0345	-0.0345	0.826	0.01305	-1.923	5.75	-2.086	2.23
4	-1.219	-1.143	-1.181	3.14	1.37	0.436	0.076	-0.038	-0.038	0.750	0.00993	-1.908	3.71	-2.338	2.15
5	-1.214	-1.139	-1.176	4.05	3.71	0.916	0.075	-0.0375	-0.0375	0.760	0.01279	-1.960	5.06	-2.249	3.49
6	-1.581	-1.512	-1.546	4.23	2.84	0.672	0.069	-0.0345	-0.0345	0.826	0.01337	-2.016	4.18	-2.200	5.35
7	-1.613	-1.548	-1.580	3.91	2.83	0.724	0.065	-0.0325	-0.0325	0.877	0.01236	-2.039	4.27	-2.224	3.55
8	-1.478	-1.407	-1.442	3.18	2.38	0.748	0.071	-0.0355	-0.0355	0.803	0.01005	-1.918	3.96	-2.129	4.98
9	-1.610	-1.535	-1.573	7.77	5.32	0.685	0.075	-0.0375	-0.0375	0.760	0.02456	-1.952	9.72	-2.173	6.37
10	-1.341	-1.275	-1.308	4.33	4.00	0.926	0.066	-0.033	-0.033	0.864	0.01368	-2.071	9.06	-2.27(sh)	-
11	-1.376	-1.311	-1.344	2.79	2.25	0.804	0.065	-0.0325	-0.0325	0.877	0.00883	-2.06(sh)	-	-2.154	10.59
12	-1.407	-1.326	-1.366	6.27	5.26	0.838	0.081	-0.0405	-0.0405	0.704	0.01984	-2.23(sh)	-	-2.533	15.53
13	-1.223	-1.154	-1.188	4.37	3.79	0.867	0.069	-0.0345	-0.0345	0.826	0.01382	-1.919	8.89	-2.07(sh)	-
14	-1.434	-1.365	-1.400	4.69	4.14	0.884	0.069	-0.0345	-0.0345	0.826	0.01482	-1.99(sh)	-	-2.090	11.70
15	-1.493	-1.424	-1.458	4.03	3.92	0.971	0.069	-0.0345	-0.0345	0.826	0.01275	-1.99(sh)	-	-2.095	11.75
16	-1.325	-1.257	-1.291	4.25	3.92	0.922	0.068	-0.034	-0.034	0.838	0.01342	-1.975	11.04	-2.09(sh)	-
17	-1.225	-1.153	-1.189	5.18	2.66	0.515	0.072	-0.036	-0.036	0.792	0.01636	-1.872	6.48	-2.01(sh)	-
18	-1.370	-1.298	-1.334	4.63	3.54	0.763	0.072	-0.036	-0.036	0.792	0.01465	-1.974	8.77	-2.146	2.41
19	-1.232	-1.159	-1.196	3.97	3.53	0.889	0.073	-0.0365	-0.0365	0.781	0.01255	-1.923	8.62	-2.02(sh)	-
20	-1.219	-1.148	-1.183	3.91	3.56	0.910	0.071	-0.0355	-0.0355	0.803	0.01236	-1.921	8.28	-2.15(sh)	-
21	-1.226	-1.154	-1.190	2.83	2.24	0.792	0.072	-0.036	-0.036	0.792	0.00895	-1.898	5.76	-	-
22	-1.213	-1.140	-1.176	3.16	2.95	0.934	0.073	-0.0365	-0.0365	0.781	0.00999	-1.915	7.08	-2.32(sh)	-
23	-1.374	-1.308	-1.341	3.88	2.51	0.647	0.066	-0.033	-0.033	0.864	0.01226	-2.064	4.45	-2.382	3.99
24	-1.382	-1.316	-1.349	3.71	3.14	0.846	0.066	-0.033	-0.033	0.864	0.01172	-2.113	3.73	-2.447	3.74

<sup>a)</sup> Substrate, 1.0 mM; (Bu<sub>4</sub>N)ClO<sub>4</sub>, 0.10M; DMF; Pt working electrode; Ag/AgNO<sub>3</sub> reference electrode; Pt wire counter electrode; 100 mV/s; r.t.;  $E_{\text{vs.}} (\text{Fe}^3/\text{Fe}^{2+})/\text{V}$ ; currents reported in  $\mu\text{A}$ . <sup>b)</sup> Estimated from  $E_{\text{pc}} - E_{\text{ox}} (-0.0285) [9]$ . <sup>c)</sup> sh = shoulder.

Table 4. Hammett *Substituent Constants*<sup>a)</sup>

	R <sup>3</sup> /R <sup>4</sup>	$\sigma_{p-x}$	$\sigma_{m-x}$	$(\sigma_{m-x} + \sigma_{p-x})/2$	R <sup>2</sup>	$\sigma_{p-x}$	$\sigma_{m-x}$	$(\sigma_{m-x} + \sigma_{p-x})/2$	$\Sigma(\sigma_{m-x} + \sigma_{p-x})/2$
<b>6</b>	H/H	0	0	0	Me	-0.17	-0.07	-0.12	-0.12
<b>7</b>	Me/H	-0.17	-0.07	-0.12	Me	-0.17	-0.07	-0.12	-0.24
<b>8</b>	F/F	0.12	0.68	0.4	Me	-0.17	-0.07	-0.12	0.28
<b>9</b>	MeO/H	-0.27	0.12	-0.075	Me	-0.17	-0.07	-0.12	-0.195
<b>10</b>	H/H	0	0	0	CF <sub>3</sub>	0.54	0.43	0.485	0.485
<b>11</b>	Me/H	-0.17	-0.07	-0.12	CF <sub>3</sub>	0.54	0.43	0.485	0.365
<b>12</b>	MeO/H	-0.27	0.12	-0.075	CF <sub>3</sub>	0.54	0.43	0.485	0.41
<b>13</b>	F/F	0.12	0.68	0.4	CF <sub>3</sub>	0.54	0.43	0.485	0.885
<b>14</b>	H/H	0	0	0	CHF <sub>2</sub>	0.32	0.29	0.305	0.305
<b>15</b>	MeO/H	-0.27	0.12	-0.075	CHF <sub>2</sub>	0.32	0.29	0.305	0.23
<b>16</b>	Cl/H	0.23	0.37	0.3	CHF <sub>2</sub>	0.32	0.29	0.305	0.605
<b>17</b>	Cl/Cl	0.46	0.74	0.6	CHF <sub>2</sub>	0.32	0.29	0.305	0.905
<b>18</b>	F/H	0.06	0.34	0.2	CHF <sub>2</sub>	0.32	0.29	0.305	0.505

<sup>a)</sup> Hammett substituent constant values are taken from [19].